Inorganic Chemistry
Article

Inorg. Chem. **2010**, *49*, 9671–9676 **9671**
DOI: 10.1021/ic101382u

Two Novel Thioindate-Thioantimonate Compounds $[Ni(dien)_2]_2In_2Sb_4S_{11}$ and $[Ni(dien)_2]_3(In_3Sb_2S_9)_2 \cdot 2H_2O$ with Transition Metal Complexes

Jian Zhou,*,† Xian-Hong Yin,‡ and Feng Zhang‡

†*Department of Chemistry and Biology, Yulin Normal University, Yulin 537000, China, and* ‡*College of Chemistry and Ecological Engineering, Guangxi University for Nationalities, Nanning 530006, China*

Received July 12, 2010

Two novel thioindate-thioantimonate compounds $[Ni(dien)_2]_2In_2Sb_4S_{11}$ (**1**) and $[Ni(dien)_2]_3(In_3Sb_2S_9)_2 \cdot 2H_2O$ (**2**) (dien = diethylenetriamine) have been solvothermally synthesized and structurally characterized. **1** contains heterometallic pseudosemicube $[In_2SbS_8]$ clusters and bow-like trimeric $[Sb_3S_7]$ units, which are linked to form a $[In_2Sb_4S_{11}^{4-}]_n$ chain, whereas **2** consists of chain-like $[In_6S_{18}]$ units and pyramidal SbS_3, which are interconnected to give a $[In_3Sb_2S_9^{6-}]_n$ layer with a large rectangle-like 12-ring. The optical properties of **1** and **2** have been investigated by UV−vis spectroscopy.

Introduction

The continuing demand for metal chalcogenides in the areas of semiconductors, catalysis, absorption, ion exchange, optical, chemical sensors, and thermoelectricity has spurred increasing interest in extending the range of framework topologies and chemical compositions[1] because the utility of these crystalline materials is intimately correlated to their geometrical features. The incorporation of other heteroatoms into the metal chalcogenide anionic framework is an effective way to enhance the structural diversity coupled with unexpected properties. In the case of thioindate, tetrahedrally coordinated metal (M) atoms (M = group 13 (Ga),[2] group 14 (Ge, Sn),[1a] and some transition metal elements[1e,3]) integrated into the $In_xS_y^{n-}$ anionic networks lead to a variety of In-M-S frameworks based on supertetrahedral clusters with tunable components and sizes as building units. However, relatively few thioindates containing other polyhedrally coordinated metal atoms have been reported.[4] The Sb^{3+} ion tends to adopt asymmetric coordination geometry (such as pyramidal SbS_3). It is expected that the combination of the In and Sb atoms in the same crystalline material may generate a new class of metal chalcogenides or thiometalates with novel structures and useful properties. But there is little research carried out on thioindate-thioantimonate compounds containing InS_4 tetrahedra and SbS_3 trigonal pyramids, only one example is a layered thioindate-thioantimonate compound $[dpaH]_5In_5Sb_6S_{19} \cdot 1.45H_2O$,[4b] where dpaH as the structure-directing agents are located at the interlayer spaces.

Recently, there has been considerable interest in the use of transition metal complexes (TMCs) as the structure-directing agents instead of organic amines or inorganic cations in synthesizing chalcogenometalates because TMCs not only have unique spatial configurations, various charges, different flexibilities, and H-bonding sites, leading to the formation of

*To whom correspondence should be addressed. E-mail: jianzhou888888@163.com.

(1) (a) Zheng, N.; Bu, X.; Wang, B.; Feng, P. *Science* **2002**, *298*, 2366–2369. (b) Sheldrick, W. S.; Wachhold, M. *Angew. Chem., Int. Ed. Engl.* **1997**, *36*, 206–224. (c) Feng, M.-L.; Kong, D.-N.; Xie, Z.-L.; Huang, X.-Y. *Angew. Chem., Int. Ed.* **2008**, *47*, 8623–8626. (d) Hsu, K. F.; Loo, S.; Guo, F.; Chen, W.; Dyck, J. S.; Uher, C.; Hogan, T.; Polychroniadis, E. K.; Kanatzidis, M. G. *Science* **2004**, *303*, 818–821. (e) Zheng, N.; Bu, X.; Feng, P. *Nature* **2003**, *426*, 428–432.

(2) Zheng, N.; Bu, X.; Feng, P. *J. Am. Chem. Soc.* **2003**, *125*, 1138–1139.

(3) (a) Bu, X.; Zheng, N.; Li, Y.; Feng, P. *J. Am. Chem. Soc.* **2002**, *124*, 12646–12647. (b) Wang, L.; Wu, T.; Zuo, F.; Zhao, X.; Bu, X.; Wu, J.; Feng, P. *J. Am. Chem. Soc.* **2010**, *132*, 3283–3285. (c) Li, H.; Kim, J.; Groy, T. L.; O'Keeffe, M.; Yaghi, O. M. *J. Am. Chem. Soc.* **2001**, *123*, 4867–4868. (d) Wang, C.; Li, Y.; Bu, X.; Zheng, N.; Zivkovic, O.; Yang, C.-S.; Feng, P. *J. Am. Chem. Soc.* **2001**, *123*, 11506–11507. Wang, C.; Bu, X.; Zheng, N.; Feng, P. *J. Am. Chem. Soc.* **2002**, *124*, 10268–10269. (e) Su, W.; Huang, X.; Li, J.; Fu, H. *J. Am. Chem. Soc.* **2002**, *124*, 12944–12945.

(4) (a) Chou, J.-H.; Kanatzidis, M. G. *Inorg. Chem.* **1994**, *33*, 1001–1002. (b) Ding, N.; Kanatzidis, M. G. *Chem. Mater.* **2007**, *19*, 3867–3869. (c) Wang, Z.; Zhang, H.; Wang, C. *Inorg. Chem.* **2009**, *48*, 8180–8185.

(5) (a) Zhang, Q.; Bu, X.; Lin, Z.; Biasini, M.; Beyermann, W. P.; Feng, P. *Inorg. Cem.* **2007**, *46*, 7262–7264. (b) Zheng, N.; Bu, X.; Feng, P. *Chem. Commun.* **2005**, 2805–2807. (c) Zhou, J.; Bian, G.-Q.; Dai, J.; Zhang, Y.; Tang, A.-B.; Zhu, Q.-Y. *Inorg. Chem.* **2007**, *46*, 1541–1543. Zhou, J.; Dai, J.; Bian, G.-Q.; Li, C.-Y. *Coord. Chem. Rev.* **2009**, *253*, 1221–1247.

(6) (a) Jia, D.-X.; Dai, J.; Zhu, Q.-Y.; Cao, L.-H.; Lin, H.-H. *J. Solid State Chem.* **2005**, *178*, 874–881. (b) Melullis, M.; Brandmayer, M. K.; Dehnen, S. *Z. Anorg. Allg. Chem.* **2006**, *632*, 64–72.

(7) (a) Pienack, N.; Näther, C.; Bensch, W. *Eur. J. Inorg. Chem.* **2009**, 1575–1577. (b) Behrens, M.; Scherb, S.; Näther, C.; Bensch, W. *Z. Anorg. Allg. Chem.* **2003**, *629*, 1367–1373. (c) Gu, X. M.; Dai, J.; Jia, D. X.; Zhang, Y.; Zhu, Q. Y. *Cryst. Growth Des.* **2005**, *5*, 1845–1848. (d) Jia, D. X.; Dai, J.; Zhu, Q. Y.; Zhang, Y.; Gu, X. M. *Polyhedron* **2004**, *23*, 937–942. (e) Pienack, N.; Lehmann, S.; Lühmann, H.; El-Madani, M.; Näther, C.; Bensch, W. *Z. Anorg. Allg. Chem.* **2008**, *634*, 2323–2329.

Published on Web 09/24/2010

a variety of unusual architectures but also can integrate the electronic, optical, and magnetic properties of TMCs with the host inorganic framework, which helps to provide complementary properties and synergistic effects.[5] So far, a number of thiogermanates,[5b,6] thiostannates,[5c,7] thioarsenates,[8] and thioantimonates[9] with the TMCs have been prepared. Lately, a few thiogallates[10] and thioindates[11] have also been prepared by using TMCs as the structure-directing agents. However, thioindate-thioantimonate compounds with the TMCs have not been reported, to the best of our knowledge. To introduce TMCs into thioindate-thioantimonate compounds and understand their role in determining the frameworks, herein we attempted to use TMCs as the structure-directing agents and successfully prepared two novel thioindate-thioantimonate compounds $[Ni(dien)_2]_2In_2Sb_4S_{11}$ (**1**) and $[Ni(dien)_2]_3(In_3Sb_2S_9)_2\cdot 2H_2O$ (**2**). The present compounds are the only examples of thioindate-thioantimonate compounds with the TMCs.

Experimental Section

General Remarks. All analytical grade chemicals were obtained commercially and used without further purification. Elemental analyses (C, H, and N) were performed using a PE2400 II elemental analyzer. Energy-dispersive X-ray analysis (EDXA) was taken by using a JEOL JSM-6700F field-emission scanning electron microscope. The UV/vis spectra were recorded at room temperature using a computer-controlled PE Lambda 900 UV/vis spectrometer equipped with an integrating sphere in the wavelength range of 250−800 nm. FT-IR spectra were recorded with a Nicolet Magna-IR 550 spectrometer in dry KBr disks in the 4000−400 cm^{-1} range. Thermogravimetric analyses (TGA) were performed using a Mettler TGA/SDTA851 thermal analyzer under a N_2 atmosphere with a heating rate of 10 °C min^{-1} in the temperature region of 30−600 °C. Powder X-ray diffraction (XRD) patterns were collected on a D/MAX-3C diffractometer using graphite-monochromatized Cu Kα radiation (λ = 1.5406 Å).

Synthesis of Compounds. Synthesis of $[Ni(dien)_2]_2In_2Sb_4S_{11}$ (1). The reagents of In (0.0012 g, 0.01 mmol), S (0.0096 g, 0.30 mmol), Sb (0.0122 g, 0.10 mmol), Ni (0.0059 g, 0.10 mmol), dien (2 mL), and H_2O (0.2 mL) were placed in a thick Pyrex tube (ca. 20 cm long). The sealed tube was heated at 180 °C for 9 days to yield yellow block-shaped crystals. The crystals were washed with ethanol, dried, and stored under vacuum (52% yield based on In). Elemental analysis. Found: C 12.09%, H 3.32%, N 10.48%; calcd C 12.02%, H 3.28%, N 10.51%. IR (cm^{-1}): 3433(m), 3218(m), 3131(m), 2917(w), 2860(w), 1575(m), 1478(m), 1326(m), 1280(m), 1165(w), 1120(w), 1043(s), 947(s), 774(m), 658(m), 576(s), 525(s), 448(m).

Synthesis of $[Ni(dien)_2]_3(In_3Sb_2S_9)_2\cdot 2H_2O$ (2). A mixture of In (0.0238 g, 0.21 mmol), S (0.0186 g, 0.58 mmol), Sb (0.0118 g, 0.09 mmol), Ni (0.0071 g, 0.12 mmol), and dien (2.3 mL) was transferred into a thick-walled Pyrex tube. The sealed tube was heated at 160 °C for 20 days to yield light red block-shaped crystals (15% yield based on In). C, H, N analysis: found C 11.12%, H 3.17%, N 9.68%; calcd C 11.16%, H 3.20%, N 9.76%. IR (cm^{-1}): 3445(m), 3253(m), 3125(m), 2920(w), 2856(w), 1581(s), 1434(m), 1319(w), 1268(w), 1165(w), 1127(w), 1050(s), 947(s), 775(m), 666(m), 582(m), 525(m), 454(m).

Crystal Structure Determination. Single-crystal X-ray diffraction data for **1** and **2** were recorded on a Rigaku Mercury CCD diffractometer using an ω-scan method with graphite monochromated Mo Kα radiation (λ = 0.71073 Å) at 293(2) K to a maximum 2θ value (50.40°). Absorption corrections were applied using multiscan technique. The structures of **1** and **2** were solved by Direct Method of SHELXS-97 and refined by full-matrix least-squares techniques using the SHELXL-97 program. Non-hydrogen atoms were refined with anisotropic temperature parameters. No H atoms associated with free water molecules in **2** were located from the difference Fourier map. The H atoms bonded to C and N atoms were positioned with idealized geometry and refined with fixed isotropic displacement parameters. SADI restraint makes all the C−C or C−N distances approximately equal. SIMU restraint prevents the thermal ellipsoids of all adjacent C and N atoms to adopt different orientations. To prevent N4, N5, and N6 atoms for **1**, and N1, S8, S9, O2a, and O2b atoms for **2** to get "nonpositive-definite" or to adopt oblate anisotropic displacement ellipsoids, these atoms were refined by a "soft" restraint with a large esd (ISOR). For **2**, Ni1, Ni2, and O2 atoms were disordered over two positions with the occupation factors of 0.66 and 0.34 for Ni1, 0.80, and 0.20 for Ni2, 0.60, and 0.40 for O2, respectively. Relevant crystal and collection data parameters and refinement results can be found in Table 1. Additional details of crystal data in CIF format can be found in the Supporting Information. Ranges of some important bond lengths and angles for **1** and **2** are listed in Table 2. The CCDC reference numbers for **1** and **2** are 793179 and 793180, respectively.

Results and Discussion

Synthesis of Thioindate-Thioantimonate Compounds. Two novel thioindate-thioantimonate compounds were obtained by the reaction of In, S, Sb, and Ni in nonstoichiometric molar ratio under solvothermal conditions. Initially, we try to prepare the thioindate-thioantimonate compounds by using the stoichiometric molar ratio of In/Sb/Ni/S in different temperature (150−190 °C), but only a yellow and gray amorphous mixture was obtained. After many experiments were made, we accidentally used the non-stoichiometric molar ratio of In/Sb/Ni/S (1/10/30/10) at 180 °C to obtain yellow crystal of **1**. According to this strategy, the quantity of In was raised and became more excessive than that of **1**, non-stoichiometric molar ratio of In/Sb/Ni/S is 21/9/58/12, which have successfully obtained **2**.

Description of the Structures. Structure of $[Ni(dien)_2]_2In_2Sb_4S_{11}$ (1). Single-crystal X-ray diffraction analysis revealed that **1** consists of one-dimensional (1-D) $[In_2Sb_4S_{11}^{4-}]_n$ anionic chains built of heterometallic pseudosemicube

(8) (a) Fu, M.-L.; Guo, G.-C.; Liu, X.; Chen, W.-T.; Liu, B.; Huang, J.-S. *Inorg. Chem.* **2006**, *45*, 5793–5798. (b) Fu, M.-L.; Guo, G.-C.; Cai, L.-Z.; Zhang, Z.-J.; Huang, J.-S. *Inorg. Chem.* **2005**, *44*, 184–186. (c) Jia, D.-X.; Zhao, Q.-X.; Dai, J.; Zhang, Y.; Zhu, Q.-Y. *Z. Anorg. Allg. Chem.* **2006**, *632*, 349–353.

(9) (a) Stephan, H.-O.; Kanatzidis, M. G. *J. Am. Chem. Soc.* **1996**, *118*, 12226–12227. (b) Vaqueiro, P.; Chippindale, A. M.; Powell, A. V. *Inorg. Chem.* **2004**, *43*, 7963–7965. (c) Kiebach, R.; Pienack, N.; Ordolff, M.-E.; Studt, F.; Bensch, W. *Chem. Mater.* **2006**, *18*, 1196–1205. (d) Schaefer, M.; Kurowski, D.; Pfitzner, A.; Näther, C.; Rejai, Z.; Möller, K.; Ziegler, N.; Bensch, W. *Inorg. Chem.* **2006**, *45*, 3726–3731. (e) Schaefer, M.; Stähler, R.; Kiebach, W.-R.; Näther, C.; Bensch, W. *Z. Anorg. Allg. Chem.* **2004**, *630*, 1816–1822. (f) Stähler, R.; Näther, C.; Bensch, W. *Eur. J. Inorg. Chem.* **2001**, 1835–1840. (g) Schaefer, M.; Näther, C.; Lehnert, N.; Bensch, W. *Inorg. Chem.* **2004**, *43*, 2914–2921. (h) Vaqueiro, P.; Darlow, D. P.; Powell, A. V.; Chippindale, A. M. *Solid State Ionics* **2004**, *172*, 601–605. (i) Stähler, R.; Bensch, W. *Eur. J. Inorg. Chem.* **2001**, 3073–3078. (j) Lühmann, H.; Rejai, Z.; Möller, K.; Leisner, P.; Ordolff, M.; Näther, C.; Bensch, W. *Z. Anorg. Allg. Chem.* **2008**, *634*, 1687–1695. (k) Stephan, H.-O.; Kanatzidis, M. G. *Inorg. Chem.* **1997**, *36*, 6050–6057. (l) Bensch, W.; Näther, C.; Stähler, R. *Chem. Commun.* **2001**, 477–478. (m) Kiebach, R.; Studt, F.; Näther, C.; Bensch, W. *Eur. J. Inorg. Chem.* **2004**, 2553–2556. (n) Stähler, R.; Bensch, W. *Z. Anorg. Allg. Chem.* **2002**, *628*, 1657–1662. (o) Powell, A. V.; Lees, R. J. E.; Chippindale, A. M. *Inorg. Chem.* **2006**, *45*, 4261–4267. (p) Stähler, R.; Mosel, B.-D.; Eckert, H.; Bensch, W. *Angew. Chem., Int. Ed.* **2002**, *41*, 4487–4489. (q) Stähler, R.; Näther, C.; Bensch, W. *J. Solid State Chem.* **2003**, *174*, 264–275.

(10) Vaqueiro, P. *Inorg. Chem.* **2006**, *45*, 4150–4156.

(11) (a) Zhou, J.; Zhang, Y.; Zhang, M.-H.; Lei, Z.-X.; Dai, J. *Z. Naturforsch.* **2009**, *64b*, 504–508. (b) Zhou, J.; Bian, G.-Q.; Zhang, Y.; Zhu, Q.-Y.; Li, C.-Y.; Dai, J. *Inorg. Chem.* **2007**, *46*, 6347–6352.

Table 1. Crystallographic Data for **1** and **2**

	1	**2**
formula	$C_{16}H_{52}In_2N_{12}Ni_2S_{11}Sb_4$	$C_{24}H_{82}In_6N_{18}Ni_3O_2S_{18}Sb_4$
Fw	1599.53	2584.33
crystal system	triclinic	orthorhombic
space group	$P\bar{1}$	*Pbcn*
a, Å	10.471(2)	25.508(5)
b, Å	14.544(3)	13.194(3)
c, Å	16.259(3)	21.653(4)
α, deg	90.52(3)	90
β, deg	91.86(3)	90
γ, deg	110.85(3)	90
V, Å^3	2312.2(8)	7287(3)
Z	2	4
T, K	293(2)	293(2)
Calcd density, Mg m^{-3}	2.297	2.352
abs coeff, mm^{-1}	4.600	4.626
F(000)	1532	4936
2*θ*(max), deg	50.40	50.20
total reflns collected	12920	32846
unique reflns	8249	6470
no. of param	427	364
$R1[I > 2\sigma(I)]$	0.0745	0.0611
*wR*2(all data)	0.1354	0.1541

$[In_2SbS_8]$ cluster and bow-like trimeric $[Sb_3S_7]$ unit, and $[Ni(dien)_2]^{2+}$ cations as counterions (Figure 1 and Supporting Information, Figure S1). The Sb atom adopts a trigonal-pyramidal SbS_3 coordination geometry. The Sb−S bond lengths and S−Sb−S bond angles are in their normal ranges. The In atom is coordinated with four S atoms to form a strong distorted tetrahedral InS_4. The observed bond lengths of In−S and bond angles of S−In−S (see Table 2) deviate severely from those of the typical tetrahedral InS_4.[2−4] This result is related to weak In···S interactions at longer distances of 2.896(5) Å for In1−S11 and 2.998(5) Å for In2−S11, which are significantly larger than the sum of the ionic radii but shorter than the sum of the van der Waals radii of In and S.[12] Taking the weak In···S bond into considerations, the coordination geometry of each In^{3+} center is in a distorted trigonal bipyramid (InS_5) with the axial bond angles, 172.10(15)° for S2−In1−S11 and 177.18(17)° for S7−In2−S11. A similar weak In···S bond is observed in $(Ph_4P)_2[InAs_3S_7]$[4a] and $[M(tren)]_4(In_2As_2S_8)_2$ (M = Mn, Zn, Co).[4c] Bond valence sums ($\sum_s = 3.03-3.09$)[13] are consistent with an oxidation state of +3 for two In atoms (In1 and In2).

Two trigonal bipyramidal InS_5 and one trigonal-pyramidal SbS_3 are joined together by edge-sharing S atoms to form a heterometallic pseudosemicube $[In_2SbS_8]$ cluster, which is closely related to semicube $[Sn_3S_{10}]$[14] or $[Sb_3S_6]$[9e,j,15] clusters. The $[Sn_3S_{10}]$ cluster is constructed by distorted trigonal bipyramidal SnS_5 units connected together via a shared axial apex and three axial−equatorial edges (Figure 2a). The backbone of the $[Sn_3S_{10}]$ cluster might be viewed as an ancestor of the $[In_2SbS_8]$ cluster, in which one SnS_5 unit of the $[Sn_3S_{10}]$ cluster is replaced by one trigonal-pyramidal SbS_3 while the remaining two SnS_5 units are replaced by two InS_5 units (Figure 2b). The further replacement of two InS_5 units of $[In_2SbS_8]$ cluster with two trigonal-pyramidal SbS_3 would lead to the formation of the $[Sb_3S_6]$ cluster (Figure 2c). Three trigonal-pyramidal SbS_3 are held together to form a bow-like trimeric $[Sb_3S_7]$ unit by corner-sharing S atoms. Notably, corner-sharing SbS_3 trigonal pyramids usually leads to dimeric saddle $[Sb_2S_5]^{4-}$,[16] cyclic $[Sb_3S_6]^{3-}$,[9m] cyclic $[Sb_4S_8]^{4-}$,[9l] and 1-D $[SbS^{2-}]_n$ or $[Sb_4S_7^{2-}]_n$ chain,[9k] but the bow-like trimeric $[Sb_3S_7]$ unit is first observed in **1**, to the best of our knowledge.

Each pseudosemicube $[In_2SbS_8]$ cluster is linked with three bow-like trimeric $[Sb_3S_7]$ units via corner-sharing S atoms and vice versa. The alternate connectivity between the $[In_2SbS_8]$ clusters and the $[Sb_3S_7]$ units by their vertices gives a 1-D $[In_2Sb_4S_{11}^{4-}]_n$ chain along the [001] direction. So far, although some 1-D thioantimonate/arsenate (III) chains containing transition metal (such as Mo, Mn, Fe, Co, Ni, Zn, Ag, Hg)[8a,b,9d−9g,17] or lanthanide metal[18] heteroatoms have been reported, main group metal heteroatoms integrated into thioantimonate/arsenate (III) anionic chain under mild solvothermal conditions are relatively rare, the limited examples include $[InAs_3S_7^{2-}]_n$,[4a] $[InAsS_4^{2-}]_n$,[4c] $[Ge_6Sb_2S_{17}^{6-}]_n$,[19] and $[Ge_2Sb_3S_{10}^{3-}]_n$.[19] The $[InAs_3S_7^{2-}]_n$ chain[4a] is composed of In^{3+} ions and $[As_3S_7]^{5-}$ units formed by corner-sharing pyramidal $[AsS_3]^{3-}$ units. The $[InAsS_4^{2-}]_n$ chain[4c] is constructed by two SbS_3 units and one $[In_2S_6]$ unit. The $[Ge_6Sb_2S_{17}^{6-}]_n$ chain[19] is formed by the interconnection of $[Ge_4S_{10}]^{4-}$ adamantane-like cluster and $[Ge_2Sb_2S_7]^{2-}$ cluster. The 1-D $[Ge_2Sb_3S_{10}^{3-}]_n$ ribbon[19] is constructed with two $[GeSbS_5^{3-}]_n$ chains bridged by Sb ions in Ψ-SbS_4 configuration. But the 1-D $[In_2Sb_4S_{11}^{4-}]_n$ chain of **1** built of the bow-like trimeric $[Sb_3S_7]$ unit and the heterometallic pseudosemicube $[In_2SbS_8]$ cluster is distinctly different from the reported chains. So the backbone of infinite anionic chain in **1** represents a new thioantimonate/arsenate (III) structural motif..

More interestingly, **1** contains *s-fac*- and *u-fac*-$[Ni(dien)_2]^{2-}$ cations as templates and charge-balancing agents (Supporting Information, Figure S2). The *u-fac*-$[Ni(3)(dien)_2]^{2-}$

(12) Hu, S.-Z.; Zhou, Z.-H.; Tsai, K.-R. *Acta Phys. Chim. Sin.* **2003**, *19*, 1073–107.
(13) Brown, I. D.; Altermatt, D. *Acta Crystallogr.* **1985**, *B41*, 244–247.
(14) (a) Jiang, T.; Lough, A. J.; Ozin, G. A.; Young, D. *Chem. Mater.* **1995**, *7*, 245–248. (b) Jiang, T.; Lough, A.; Ozin, G. A.; Bedard, R. L.; Broach, R. *J. Mater. Chem.* **1998**, *8*, 721–732. (c) Jiang, T.; Lough, A.; Ozin, G. A. *Adv. Mater.* **1998**, *10*, 42–46. (d) Parise, J. B.; Ko, Y.; Rijssenbeek, J.; Nellis, D. M.; Tan, K.; Koch, S. *J. Chem. Soc., Chem. Commun.* **1994**, 527–528. (e) Ko, Y.; Tan, K.; Nellis, D. M.; Koch, S.; Parise, J. B. *J. Solid State Chem.* **1995**, *114*, 506–511. (f) Jiang, T.; Lough, A. J.; Ozin, G. A.; Young, D. *Chem. Mater.* **1995**, *7*, 245–248.
(15) (a) Puls, A.; Schaefer, M.; Näther, C.; Bensch, W.; Powell, A. V.; Boissière, S.; Chippindale, A. M. *J. Solid State Chem.* **2005**, *178*, 1171–1181. (b) Kiebach, R.; Griebe, A.; Näther, C.; Bensch, W. *Solid State Sci.* **2006**, *8*, 541–547. (c) Spetzler, V.; Kiebach, R.; Näther, C.; Bensch, W. *Z. Anorg. Allg. Chem.* **2004**, *630*, 2398–2404. (d) Parise, J. B.; Ko, Y. *Chem. Mater.* **1992**, *4*, 1446–1450. (e) Lees, R. J. E.; Powell, A. V.; Chippindale, A. M. *Acta Crystallogr.* **2005**, *C61*, m516–m518. (f) Wang, X.; Liu, L.; Jacobson, A. J. *J. Solid State Chem.* **2000**, *155*, 409–416.
(16) Jia, D.-X.; Zhang, Y.; Dai, J.; Zhu, Q.-Y.; Gu, X.-M. *J. Solid State Chem.* **2004**, *177*, 2477–2483.
(17) (a) Kiebach, R.; Bensch, W.; Hoffmann, R.; Pöttgen, R. *Z. Anorg. Allg. Chem.* **2003**, *629*, 532–538. (b) Chou, J. H.; Kanatzidis, M. G. *Chem. Mater.* **1995**, *7*, 5–8. (c) Kong, D.-N.; Xie, Z.-L.; Feng, M.-L.; Ye, D.; Du, K.-Z.; Li, J.-R.; Huang, X.-Y. *Cryst. Growth Des.* **2010**, *10*, 1364–1372. (d) Wang, X.; Sheng, T.-L.; Hu, S.-M.; Fu, R.-B.; Chen, J.-S.; Wu, X.-T. *J. Solid State Chem.* **2009**, *182*, 913–919. (e) An, Y.; Li, X.; Liu, X.; Ji, M.; Jia, C. *Inorg. Chem. Commun.* **2003**, *6*, 1137–1139. (f) Chou, J.-H.; Hanko, J. A.; Kanatzidis, M. G. *Inorg. Chem.* **1997**, *36*, 4–9.
(18) (a) Wu, Y.; Näther, C.; Bensch, W. *Inorg. Chem.* **2006**, *45*, 8835–8837. (b) Jia, D.-X.; Deng, J.; Zhao, Q.-X.; Zhang, Y. *J. Mol. Struct.* **2007**, *833*, 114–120. (c) Jia, D.-X.; Zhu, Q.-Y.; Dai, J.; Lu, W.; Guo, W.-J. *Inorg. Chem.* **2005**, *44*, 819–821. (d) Jia, D.; Zhao, Q.; Zhang, Y.; Dai, J.; Zuo, J. *Inorg. Chem.* **2005**, *44*, 8861–8867.
(19) Feng, M.-L.; Xiong, W.-W.; Ye, D.; Li, J.-R.; Huang, X.-Y. *Chem. Asian J.* **2010**, *5*, 1817–1823.

Table 2. Ranges of Some Important Bond Lengths (Å) and Angles (deg) for **1** and **2**

1

In1−S	2.441(5)−2.896(5)	In2−S	2.455(5)−2.998(5)
Sb1−S	2.388(5)−2.492(5)	Sb2−S	2.337(6)−2.457(5)
Sb3−S	2.386(5)−2.494(5)	Sb4−S	2.399(5)−2.436(5)
Ni1−N	2.085(13)−2.166(14)	Ni2−N	2.052(16)−2.134(15)
Ni3−N	2.025(15)−2.135(18)		
S−In1−S	82.45(17)−172.10(15)	S−In2−S	80.81(17)−177.18(17)
S−Sb1−S	91.71(16)−99.57(17)	S−Sb2−S	95.93(18)−104.15(17)
S−Sb3−S	90.50(18)−98.75(18)	S−Sb4−S	94.68(18)−103.6(2)
N−Ni1−N(cis)	81.0(5)−99.0(5)	N−Ni1−N(trans)	180.0(4)
N−Ni2−N(cis)	81.0(6)−99.0(6)	N−Ni2−N(trans)	180.0(9)
N−Ni3−N(cis)	80.0(6)−96.1(6)	N−Ni3−N(trans)	168.7(6)−172.9(7)

2

In1−S	2.429(3)−2.473(3)	In2−S	2.444(3)−2.470(3)
In3−S	2.424(4)−2.486(5)	Sb1−S	2.427(3)−2.437(3)
Sb2−S	2.415(5)−2.432(4)	Ni1−N	1.992(16)−2.310(17)
Ni2−N	2.056(16)−2.149(15)		
S−In1−S	105.25(12)−115.04(11)	S−In2−S	102.00(13)−116.97(12)
S−In3−S	94.55(15)−116.1(2)	S−Sb1−S	94.54(11)−99.15(11)
S−Sb2−S	94.14(17)−115.04(11)		
N−Ni1−N(cis)	80.1(8)−99.2(9)	N−Ni1−N(trans)	163.3(6)−175.3(10)
N−Ni2−N(cis)	79.7(6)−103.8(6)	N−Ni2−N(trans)	165.5(6)−172.7(6)

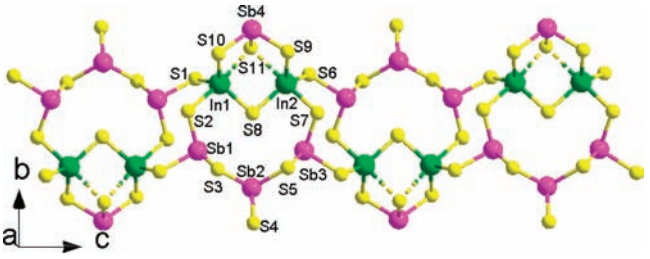

Figure 1. $[In_2Sb_4S_{11}^{4-}]_n$ anionic chain in **1**.

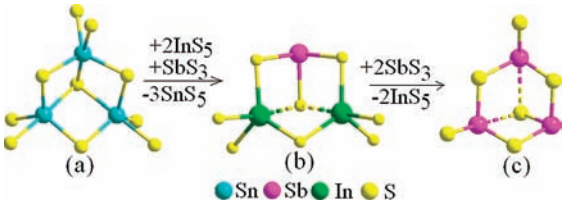

Figure 2. View of structures: (a) $[Sn_3S_{10}]$, (b) $[In_2SbS_8]$, and (c) $[Sb_3S_6]$.

cations are located between the parallel anionic chains and form extensive N−H···S H-bonds with the S atoms of the anionic chain, resulting in a 2-D layered arrangement parallel to the (001) plane (Supporting Information, Figure S3). These layers are further stacked in an -AAA- fashion along the *b* axis. The *s-fac*-$[Ni(1, 2)(dien)_2]^{2-}$ cations reside in the interlayer spaces and interact with the S atoms of the adjacent layers by N−H···S H-bonds to give an overall 3-D supramolecular architecture (Figure 3). The N···S distances and the N−H···S angles are in accordance with the values reported in the literature.[4c]

Structure of $[Ni(dien)_2]_3(In_3Sb_2S_9)_2\cdot 2H_2O$ (2). 2 consists of two-dimensional (2-D) $[In_3Sb_2S_9]^{6-}$ anionic layers, charge compensating $[Ni(dien)_2]^{2+}$ cations, and free water molecules (Figure 4a and Supporting Information, Figure S4). The 2-D $[In_3Sb_2S_9]^{6-}$ anionic layer is built up from unusual chain-like $[In_6S_{18}]$ unit and $[SbS_3]$ unit. The In^{3+} ion is coordinated with four S atoms to form a slightly distorted tetrahedral InS_4. The Sb^{3+} ion adopts a SbS_3 trigonal-pyramidal

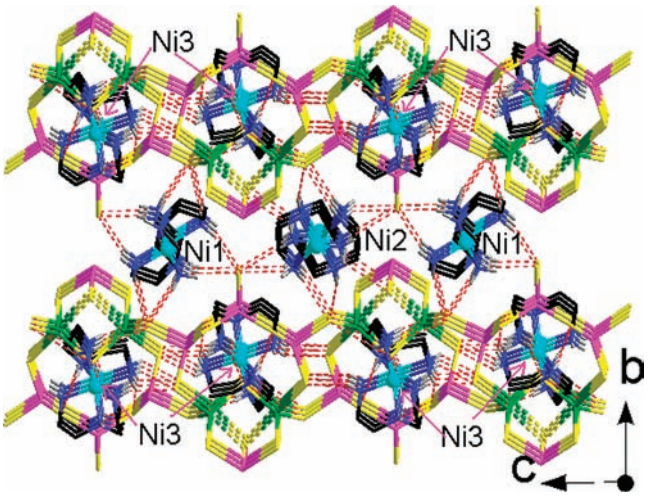

Figure 3. 3-D supramolecular architecture constructed by N−H···S H-bonds. H atoms bonded to C atoms have been omitted for clarity.

coordination geometry. Two InS_4 tetrahedra are connected via one corner to form a In_2S_7 unit. Two InS_4 tetrahedra share a common edge to give a In_2S_6 unit with a planar four-membered In_2S_2 ring. Two In_2S_7 units and one In_2S_6 unit are joined together by corner-sharing S atoms to form a chain-like $[In_6S_{18}]$ secondary building unit (SBU) with a center of inversion (Figure 4b). There are three kinds of In···In distances in $[In_6S_{18}]$ SBU, 3.814 Å for In1···In2, 3.686 Å for In2···In3, and 3.308 Å for In3···In3A (symmetry operation: (A) $1-x, 1-y, -z$), compared with those (3.3−3.9 Å for In···In distance) in $[(C_3H_7)_2NH_2]_3In_6S_{11}H$.[20] Notably, SBUs based on the combination of corner- and edge-sharing InS_4 tetrahedra are very scarce, mainly because corner-sharing InS_4 tetrahedra tends to form supertetrahedral clusters, such as T_2 cluster $[In_4S_{10}]^{8-}$,[21] T_3 cluster $[In_{10}S_{20}]^{10-}$,[2] T_4 cluster $[M_4In_{16}S_{33}]^{10-}$ (M = Mn, Co, Zn,

(20) Cahill, C. L.; Gugliotta, B.; Parise, J. B. *Chem. Commun.* **1998**, 1715–1716.
(21) Krebs, B.; Voelker, D.; Stiller, K. *Inorg. Chim. Acta* **1982**, *65*, L101–L102.

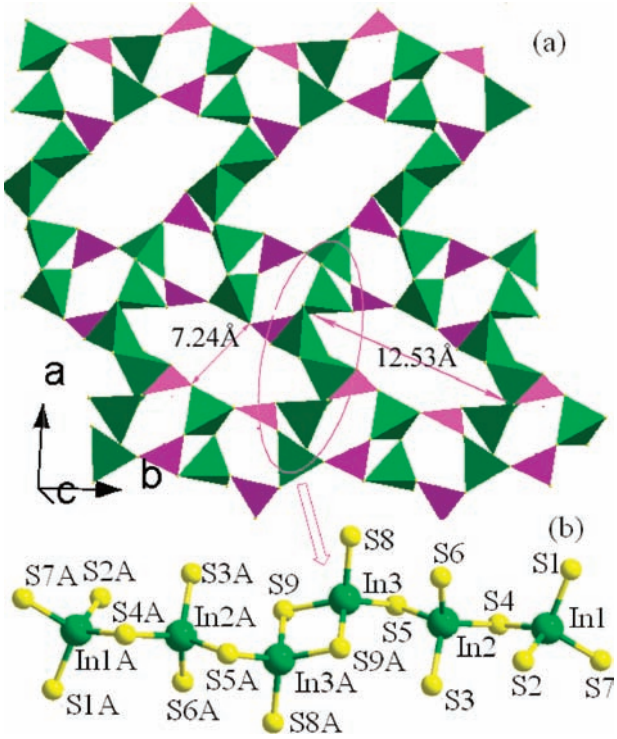

Figure 4. (a) Polyhedral view of a $[In_3Sb_2S_9]^{6-}$ layer, green tetrahedra are InS_4 units, and magenta trigonal pyramids are SbS_3 units in **2**. (b) The chain-like $[In_6S_{18}]$ secondary building unit. [Symmetry operation: (A) $1-x$, $1-y$, $-z$].

Cd),[3d] and T_5 cluster $[Cu_5In_{30}S_{54}]^{13-}$,[3a] and edge-sharing InS_4 tetrahedra easily forms 1-D $[InS_2^-]_n$ chains.[11b] So the chain-like $[In_6S_{18}]$ SBU based on the combination of corner- and edge-sharing InS_4 tetrahedra is first observed in **2**.

In **2**, each chain-like $[In_6S_{18}]$ SBU is linked to eight adjacent SbS_3 trigonal pyramids by corner- and edge-sharing S atoms, resulting in a 2-D anionic layer of $[In_3Sb_2S_9]^{6-}$ parallel to the (001) plane. The 2-D network of **2** features a puckered layer with rectangle-like 12-ring delimited by eight InS_4 tetrahedra and four SbS_3 trigonal pyramids. The larger 12-ring has a window size of 7.24×12.53 Å^2 as measured using the interatomic distances. These layers are stacked in an -AAA- fashion along the *c* axis to form 1-D tunnel-like features (Figure 5). The interlayer distance is estimated to be 15.45 Å. Above and below these 12-rings reside the $[Ni(dien)_2]^{2-}$ cations which are normal chelate complexes of Ni^{2+} ions with dien ligands in both mer- (Ni1) and *s*-fac- (Ni2) conformations (Figure 6 and Supporting Information, Figure S5). Distances between N atoms in $[Ni(dien)_2]^{2-}$ and S atoms in the anionic layer lie in the range 3.212(16)−3.704(17) Å, suggesting a N−H···S H-bonding interaction between the cations and the anionic layers.[4c]

Although the layers of **2** and reported $[dpaH]_5In_5Sb_6S_{19}\cdot 1.45H_2O$[4b] are built from InS_4 tetrahedra and SbS_3 pyramids, the structures are completely different (Supporting Information, Figure S6). The first is that different binding modes of InS_4 tetrahedra lead to different $[In_xS_y]$ SBU: in the $[In_5Sb_6S_{19}]^{5-}$ layer, corner-sharing InS_4 tetrahedra result in two SBUs, namely, dimeric $[In_2S_7]$, and trimeric $[In_3S_{10}]$ units, whereas corner- and edge-sharing InS_4 tetrahedra in the $[In_3Sb_2S_9]^{6-}$ layer lead to the chain-like $[In_6S_{18}]$ unit. The second is a different shape of large

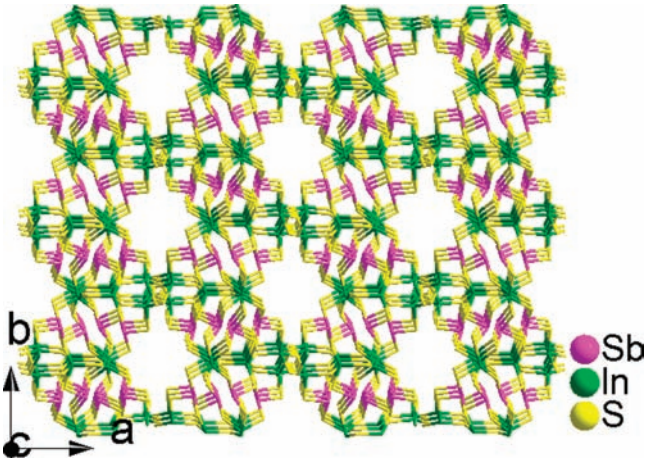

Figure 5. $[In_3Sb_2S_9]^{6-}$ layers stacked in an -AAA- fashion along the *c* axis, showing 1-D tunnel-like features. The $[Ni(dien)_2]^{2+}$ cations and free water molecules have been omitted for clarity.

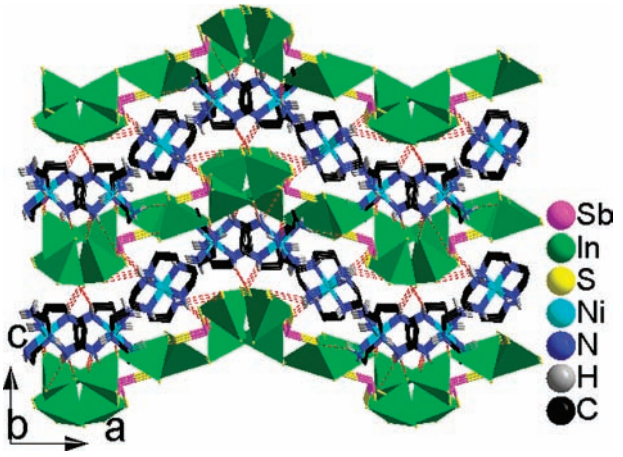

Figure 6. 3-D supramolecular framework linked by N−H···S H-bonds, showing the -AAA- stacking modes (the indium tetrahedra are shaded in green). H atoms bonded to C atoms and free water molecules have been omitted for clarity.

12-ring and layer: Polymeric $[In_5Sb_6S_{19}]^{5-}$ anion displays the slab layer with elliptical 12-ring delimited by six InS_4 and six SbS_3, while the $[In_3Sb_2S_9]^{6-}$ anion exhibits the puckered layer with rectangle-like 12-ring delimited by eight InS_4 and four SbS_3. The formation of two different layers could be related to the different charge balancing cations as the structure-directing agents.

Optical diffuse reflection spectra of **1** and **2** were measured at room temperature (Supporting Information, Figure S7). The absorption (α/S) data were calculated from the reflectance using the Kubelka−Munk function.[22] The optical band gaps obtained by extrapolation of the linear portion of the absorption edges are estimated as 3.39 eV for **1**, and 3.04 eV for **2**, which can be assigned to the electronic excitation of the anion. These band gaps were close to those of other indium sulfides $[Ni(tepa)]_2[In_4S_7(SH)_2]\cdot H_2O$ (3.28 eV)[11b] and $[In_8S_{13}(S_3)_{1/2}(SH)][In_4S_6(S_3)_{1/2}(SH)]\text{-}(TMDPH_2)_5$ (3.1 eV),[23] showing that **1** and **2** are wide-band gap semiconductors.

(22) Wendlandt, W. W.; Hecht, H. G. *Reflectance Spectroscopy*, Wiley-Interscience: New York, 1966.
(23) Zhang, Q.; Bu, X.; Han, L.; Feng, P. *Inorg. Chem.* **2006**, *45*, 6684–6687.

In conclusion, two novel thioindate-thioantimonate compounds with TMCs have been synthesized under mild hydrothermal conditions. Besides providing the only examples of thioindate-thioantimonate compounds with TMCs, different binding modes of InS_4 tetrahedra and SbS_3 trigonal pyramids lead two different In−Sb−S frameworks, which reflects the structure-directing influence of different conformation of the cations (*u-fac*-$[Ni(3)(dien)_2]^{2-}$ for **1** and *mer*-$[Ni(1)(dien)_2]^{2-}$ for **2**). The successful synthesis of **1** and **2** provides possibilities of making other novel thioindate-thioantimonate compounds with structural diversity and interesting optical and electronic properties by TMCs as the structure-directing agents. Further research on this subject is in progress.

Acknowledgment. This work was supported by the NNSF of Chain (Grant 20961011), China Postdoctoral Science Foundation (Grant 20090450183), the NSF of Guangxi Province (Grant 2010GXNSFB013017) and the NSF of the Education Committee of Guangxi Province. The authors are also grateful to Yulin Normal University for financial support.

Supporting Information Available: Crystal data in CIF format, IR data, XRD data, and TG curve. This material is available free of charge via the Internet at http://pubs.acs.org.